Review

Recent advances in organometallic electrochemistry

Fernando Battaglini [a,*], Ernesto J. Calvo [a,1], Fabio Doctorovich [b]

[a] *Departamento de Química Inorgánica, Analítica y Química Física, Facultad de Ciencias Exactas y Naturales, Universidad de Buenos Aires, Ciudad Universitaria— Pabellón 2, 1428 Buenos Aires, Argentina*
[b] *Departamento de Química Orgánica, Facultad de Ciencias Exactas y Naturales, Universidad de Buenos Aires, Ciudad Universitaria— Pabellón 2, 1428 Buenos Aires, Argentina*

Received 2 December 1996

Abstract

Recent advances in electrochemistry are presented as a tool for mechanistic studies and synthesis of organometallic compounds. Special attention is given to the use of microelectrodes, ultrafast cyclic voltammetry, spectroelectrochemistry and digital simulation for mechanistic and thermodynamic studies. Electrochemically initiated electron transfer chain catalysis is discussed as a synthetic method for selective substitution in clusters and binuclear compounds. The synthesis of organometallic compounds using sacrificial electrodes and the electrochemical generation of organometallic catalysts useful in organic synthesis are presented. © 1997 Elsevier Science S.A.

1. Introduction

The use of electrochemical methods for studying the mechanism of electron transfer (ET) to obtain thermo-dynamic data and for the synthesis of organometallic complexes has been known since the early work of Page and Wilkinson [1]. From the late 1970s, organometallic compounds have generated a series of new electrodes by modification of their surfaces with monolayers [2] or electroactive polymeric materials [3]. Some of them have found electroanalytical uses [4,5]. A comprehensive review of the electrochemistry of organometallic compounds was written by Morris [6] in 1974. Since then, the field has grown exponentially and reviews devoted to particular areas of this field have appeared. Among them it is worth mentioning the reviews by De Montauzon et al. [7] and Connelly and Geiger [8] on electrochemistry of transition metal organometallic compounds, the relation between photochemical and electrochemical activation [9], solution ET reactions in organometallic electrochemistry [10], the aid of electrochemistry in deducing structures combined with spectroscopic techniques [11], electrochemical synthesis of organometallic compounds [12] and the periodical reviews of Analytical Chemistry on Dynamic Electrochemistry, the last one from 1994 [13]. We attempt to cover the period 1980–1995 with special emphasis in the advances of electrochemical techniques useful in organometallic electrochemistry, the electrosynthesis of organometallic compounds, their use as catalysts in electrochemical synthesis and the application of organometallics in modified electrodes.

2. Electrochemical methods

Several electrochemical techniques are used in the synthesis and study of organometallics. Cyclic voltammetry (CV), polarography, chronoamperometry and coulometry are among the most used. These were well-established methods by 1980, and there are existing excellent texts [14–16] and articles [7,17] describing their theoretical background. Some of the major innovations in electrochemical techniques in the 1980s were: the use of electrodes with diameter less than $50 \mu m$, called microelectrodes; the development of ultrafast CV; new advances in spectroelectrochemistry; the popularization of digital simulation of electrochemical processes as a tool to elucidate reaction mechanisms. A brief description of their advantages and theoretical background are given.

2.1. Microelectrodes and ultrafast CV

Microelectrode techniques have been utilized increasingly in electrochemistry since the advantages of low

---

* Corresponding author. Tel.: (+54) 1 7828843; fax: (+54) 1 7320441; e-mail: battagli@nahuel.q1.fcen.uba.ar.
[1] Also corresponding author.

dimensioned electrodes began to be realized. Many of the undesirable aspects of electrochemical techniques, namely uncompensated resistance in non-aqueous solvents and mass transport limitations, are reduced with microelectrodes. Moreover, microelectrodes are easily implemented and involve relatively low costs. Therefore, a growing number of laboratories are applying microelectrode techniques to investigate a wide variety of problems in diverse systems, some of them not accessible with conventional, larger electrodes. The purpose of this section is to describe the most remarkable features, theoretical background and some experimental aspects on microelectrodes. Further information can be found elsewhere [16,18,19].

Three major consequences arise from the reduction in size of an electrode: (1) mass transport rates to and from the electrode are increased because of non-linear diffusion; (2) the double layer capacitance is reduced due to the reduction in electrode surface; (3) ohmic drops, which are the product of electrode current and solution resistance, are reduced due to the low current and geometry-dependent resistance.

In particular, the use of microelectrodes in CV has the following effects. (1) At conventional scan rates (less than $2\,V\,s^{-1}$) a current plateau is observed (Fig. 1(a)) instead of a peak since the behavior is closer to a spherical electrode than a planar electrode. When a very fast scan rate is used, the diffusion layer is thin and the behavior is equivalent to linear diffusion. Then, the shape of the voltammogram is similar to a conventional CV (Fig. 1(b)). (2) Since ohmic drop and double layer capacitance are reduced, higher scan rates can be achieved. This reduces the time scale available for this type of experiment and meaningful CV at scan rates approaching $10^6\,V\,s^{-1}$ has been established. This allows the measurement of heterogeneous ET rate constants in the range of centimeters per second or homogenous rate constants corresponding to submicrosecond lifetimes [20].

Another major advantage of microelectrodes is that as currents are small, ohmic drop is also small. This allows the use of organic solvents of high resistance

such as benzene or toluene. Bond et al. [21] have used these solvents, with tetrahexylammonium salts as supporting electrolytes, to study the $[Cr(CO)_2(Ph_2PCH_2CH_2PPh_2)]^{+/0}$ system. The principles of the use of microdisk electrodes in high-resistance media have been reviewed by Heinze [22].

Owing to the low currents, it is possible to avoid the addition of supporting electrolyte to the solvents. Therefore, the positive limit of some non-aqueous solvents can be considerably extended since this limit is frequently due to reactions of the added electrolyte anion. This allowed, for example, the study of the anodic oxidation of methane, butane and other aliphatic alkanes in acetonitrile at potentials up to ca. $4.3\,V$ versus Ag/Ag^+ [23].

Conventional potentiostatic control with three-electrode cells is generally not necessary due to the low currents and the reference electrode serves also as counter electrode. Potentiostatic control is usually achieved by applying the potential directly to the reference/counter electrode. The currents are measured with a high gain picoammeter or purpose-built current follower connected in series with the cell.

The main source of noise in the measured current is due to capacitive coupling resulting from the high impedance of the microelectrode. Therefore, it is important to electrically shield the cell and its connections from external sources of a.c. voltage. This can be achieved by enclosing the electrochemical cell in a Faraday cage and using low noise coaxial cable to connect it with the waveform generator and picoammeter. Details on the instrumentation are found elsewhere [24–27].

2.2. Digital simulation in electrochemistry

The rate of an electrochemical reaction is governed by the rate of mass transport and the homogeneous reactions coupled to the heterogeneous ET. In some cases, it is possible to solve the differential equation that describes the chemical reactions and the mass transfer. However, in most cases the analytical solution is impossible to obtain. In these cases numerical methods are used. The applied model consists of dividing the solution of an electrolyte into elements of small and discrete volume. In each element the electrolyte concentration is regarded as constant. Since these methods are implemented on a digital computer and a model of the electrochemical system is allowed to evolve by means of algebraic equations, a digital simulation of the experiment is carried out.

The simplest model is to consider linear diffusion to the electrode surface, since the concentration in each box only changes in the normal direction to the electrode surface. For microelectrodes, or when a convec-
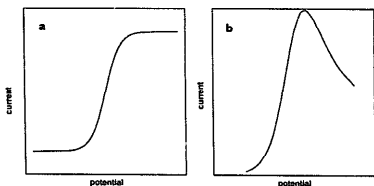

Fig. 1. Shape of voltammograms for (a) microelectrode at slow scan rates, (b) for a conventional electrode or a microelectrode at very fast scan rates (linear diffusion).

tive process is added, the model becomes more complex, but can be treated.

For linear diffusion the solution is represented by a series of boxes extending away from the electrode surface (Fig. 2). The electrode surface is in the center of the first box and each box j characterizes the solution at a distance $x = (j - 1)\Delta x$ from the interface. If A is the species in solution, its concentration in each box is denoted as $C_A(j)$. In this way the discrete model with a concentration array describes closely the continuous system. Δx is a variable of the model. The smaller is Δx, the more elements are needed in the array and the model becomes more refined.

The diffusion process and the possible coupled chemical reactions change the concentrations of the species in solution in each time step. Therefore it is necessary to discretize the time variable in small intervals Δt.

To model the system, the equations which describe the mass transfer process and the chemical reactions must be written in an algebraic form that consider the changes in an interval Δt. These equations are applied to the concentration arrays that describe the initial system.

The first application transforms the arrays in a new set of data which can be seen as the evolution of the system at a time Δt. The second application characterizes the system at a time $2\Delta t$ and so on. The evolution in time of the digital model approaches the real system as Δt is decreased.

Digital simulation allows treatment of the interplay of diffusion, homogeneous kinetics and convection that accompany heterogeneous ET processes at electrodes of particular geometry under a given potential or current perturbation.

The pioneer of digital simulation in electrochemistry is Feldberg, who in 1964 co-wrote his first article on this subject [28]. Today, the fundamental reference for digital simulation in electrochemistry is the article by Feldberg in 'Electroanalytical Chemistry: A Series of Advances' [29], in which he describes the box method. A more recent text on this subject is the book by Britz [30]. Heinze and co-workers wrote a series of papers dealing with digital simulation of microelectrodes for different electrochemical techniques [31–33]. Also, commercial software for digital simulation of electrochemical processes is available [34,35]. A review on commercial software applied to CV can be found in Ref. [36].

Fig. 2. Discrete model of the solution in an electrochemical experiment considering only linear diffusion.

The use of digital simulation in the study of reaction mechanisms has proved to be very useful. This will be discussed in a later section, especially those involving a several steps mechanism in organometallic electrochemistry.

2.3. Spectroelectrochemistry

Spectroscopic detection of reaction intermediates produced by electrochemical methods has increasingly been used in organometallic chemistry by UV–visible, infrared and electron spin resonance (ESR) spectroscopies simultaneously with electrolysis. Reviews on spectroelectrochemistry are available [37–39].

Among the aspects to be considered when designing a spectroelectrochemical experiment are: mass transport conditions; time scale of detection and integration when short-lived intermediates are involved; the sensitivity limit of the spectroscopic techniques under the conditions of the electrochemical experiment. Hydrodynamic electrodes such as channel electrodes have been specifically designed for use with spectroscopic techniques in relation to concentration gradients and diffusion. Finally, it is always important to match both the experimental conditions for spectroscopic and electrochemical experiments, which are usually in conflict.

Optically transparent electrodes (OTEs) operate in the semi-infinite diffusion regime. They consist of a transparent conductive electrode sandwiched in the optical path, thus operating in the transmission mode. From the Lambert–Beer law, the absorbance is given by integration of all absorbing molecules in the optical path. The time dependence of the absorbance A can be obtained from the Cottrell semi-infinite diffusion equation:

$$A(\lambda,t) = \frac{2C_0^\infty \varepsilon(\lambda) D^{1/2} t^{1/2}}{\pi^{1/2}} \quad (1)$$

where D is the diffusion coefficient of the reactant or intermediate O, produced or consumed at the transparent electrode, C^∞ is its bulk concentration, $\varepsilon(\lambda)$ is the absorptivity at wavelength λ and t is time.

Since it is possible to record the A vs. t response with a resolution of 5–10 ms it is possible to obtain bimolecular rate constants as high as 10^8 to 10^9 dm^3 mol^{-1} s^{-1}. The limit is given by the rise time of the potential perturbation or the time constant of the cell (limited by the RC with R the solution resistance and C the double layer capacitance).

For complex reaction mechanisms involving chemical steps, rate constants can be obtained by comparison of the experimental absorbance transient with digital simulation for a given kinetic scheme. Reilley and co-workers have analyzed many different mechanisms using double-potential step chrono-absorptiometry [40].

A variation of the potential transient is the 'switch off' or open circuit relaxation (OCR) experiment, in which after a fixed potential is applied for some time the electrical circuit is opened. Then, the absorbance is monitored while allowing chemical relaxation of the species electrochemically formed. For complex reactions where the concentration decay equation cannot be obtained in analytical closed form, analysis of the experimental transient in the Laplace space [41] allows rate constants to be obtained.

Optically transparent thin-layer electrodes (OTTLEs) were introduced by Murray et al. in 1967 [42]. This technique consists of a noble metal minigrid sandwiched between two glass plates entrapping electrolyte in the light path. OTTLE cells are sufficiently small to fit in a conventional spectrophotometer in the UV–visible and complete electrolysis can be achieved in 30–60 s due to the thin electrolyte layer. By controlling the electrode potential, very reactive intermediates can be isolated and identified spectroscopically free from residual details of redox chemical reagents.

In addition, the number of faradays exchanged per mole of intermediate being formed can be obtained by extensive or complete electrolysis and coulometry since the charge and concentration changes can be quantified.

Spectroelectrochemical mediator titration can be used to determine formal potentials and the number of electrons n involved in the reaction, as currently done in bio-inorganic chemistry with redox proteins. This can be compared to the method developed by Pugh and Meyer [43] (vide infra).

An important drawback of OTTLEs in transient studies, however, is their poor time response due to the high resistance of the thin electrolyte layer. They are better suited for the study of species with long half-lives that cannot be studied with OTEs because of convection limitations.

Combination of an OTTLE and hydrodynamic electrode [44] is the channel electrode geometry developed by Compton and Wellington [45]. A semi-transparent minigrid electrode mounted within a thin layer silica cell with the reference electrode upstream and the counter electrode downstream. The electrolyte can be flowed through the cell, and electrolysis under UV–visible irradiation could be carried out under steady state conditions. The absorption spectrum of electrogenerated species can be recorded at different flow rates or the absorbance at constant wavelength can be recorded under electrochemical perturbation.

The precise knowledge of the convective flow for this geometry permits the quantitative modeling of mass transport within the cell and the concentration as a function of cell length perpendicular to the optical path. This makes it possible to carry out kinetic studies spectroscopically on the electrochemical intermediates as well as identify them by new spectra.

An extension of this set-up for electro-fluorimetric measurements of electrogenerated species could be realized [45].

Electrochemical flow OTTLE cells have been used in combination with UV–visible as well as ESR spectroscopies by Compton and co-workers [46,47]. In the latter case the electrochemical ESR signal could be described to follow a dependence on the length in the direction of flow given by the convolution of the cavity sensitivity function and the concentration decay if the electrode was positioned just above the cavity.

In situ electrochemical ESR provides a very sensitive method to detect paramagnetic species, such as intermediates of one-electron electrode reactions. In addition, electrochemical ESR can be used to follow reaction kinetics. Initially it was introduced for electrochemical generation of radical species just above the ESR cavity. Highly resolved ESR spectra can be obtained by freezing the electrolyzed solution. For a review on electrochemical ESR see Ref. [48]. ESR electrochemical cells under electrolyte flowing conditions are useful to detect short-lived intermediates if a paramagnetic signal can be detected at room temperature under steady state conditions. For the shortest lived intermediate species that can be annihilated during the transit from the generator electrode to the ESR cavity, in situ experiments with the electrode inside the cavity at high flow rate are better suited. This requires careful positioning of the electrode in the cavity at a node of the standing wave.

Hydride-forming catalyst intermediates (bpy)M(C$_n$R$_n$) with M = Rh, Ir ($n = 5$); M = Ru, Os ($n = 6$) undergo two-electron reduction, chemically or electrochemically, with formation of highly colored unsaturated species. Stable hydride intermediates of these catalyst were isolated and characterized for 5d systems [(bpy)MH(C$_n$R$_n$)]$^+$, with M = Ir ($n = 5$) and Os ($n = 6$). They can be reversibly reduced to neutral radical complexes as shown by resolved ESR spectra [49].

Other recent examples of in situ simultaneous ESR and electrochemistry are the papers of Bond and co-workers on the oxidation of mer/fac-Cr(CO)$_3$(η^1-L–L)(η^2-L–L) [50] and Ghilardi et al. on [Me{(PPh$_2$CH$_2$)$_3$CMe}(o-S$_2$C$_6$H$_4$)]$^{n+}$, with M = Fe, Co or Rh and $n = 0$ or 1 [51].

Du Bois and Turner pioneered the field of FTIR spectroelectrochemistry in organometallics. They studied Mo(N$_2$)$_2$(PPh$_2$Me)$_2$ with an OTTLE [52]. Instead of the conventional stagnant cell, Roth and Weaver developed a thin-layer spectroelectrochemical cell with forced hydrodynamic flow to study adsorbed species in situ [53].

Mann and co-workers studied the IR spectroelectrochemistry of substituted phosphine complexes, XTa(CO)$_4$(dppe) (X = I,Br) and XM(CO)$_2$(dppe)$_2$ (where dppe is 1,2-bis(diphenylphosphino)ethane; X = H, I, Br, Cl; M = Nb,Ta) with a thin layer cell [54].

Characterization of the electrochemically generated radical cations $ClNb(CO)_2(dppe)_2^+$ and $HNb(CO)_2(dppe)_2^+$ was also achieved by ESR spectroscopy.

Weaver and co-workers [55] explored the IR spectroelectrochemical properties of several high nuclearity Pt carbonyl clusters in dichloromethane. The three Pt clusters $[Pt_{24}(CO)_{30}]^{n-}$, $[Pt_{26}(CO)_{32}]^{n-}$ and $[Pt_{38}(CO)_{44}]^{n-}$ ($n = 0$ to 6) exhibit a sequence of fast ET reactions at electrodes with net charges from 0 to 10. Simultaneous FTIR spectroelectrochemistry shows that the C–O stretching frequency decreases systematically as n becomes more negative (for Pt_{24} it decreases 15–$20\,cm^{-1}$ per added electron).

A good example of combination of several spectroelectrochemical techniques applied to organometallic chemistry is the work of Kaim and co-workers [56]. By combination of CV, IR, OTTLE UV–vis–near-IR, and ESR spectroscopies the authors elucidated the electronic structure of the 16-valence electron fragments $M(CO)_3(PR_3)_2$ (M = Mo, W; R = isopropyl, cyclohexyl) in their complexes with H_2, THF and three p-conjugated dinucleating ligands.

3. Mechanistic and kinetic studies

In recent years more complex mechanisms could be studied with the aid of digital simulation and the combination of electrochemical techniques with spectroscopic methods. Microelectrodes and ultrafast CV were used to detect short-lived species. Some examples are presented in the use of these techniques to understand ET mechanisms in organometallic compounds.

Generally, the electrode reaction is combined with other homogeneous reactions. The types of chemical reaction that are encountered as steps in organometallic electrode reactions are extremely diverse. A given reaction can be protonation, deprotonation, bond cleavage, complexation or decomplexation, ligand exchange, nucleophilic or electrophilic attack, homogeneous ET, isomerization, conformational change, etc.

Reactions that occur at the electrode surface are named electrochemical (E) and those that occur in solution are named chemical (C). Thus, the different steps involved in a given mechanism can be classified as E or C. Their combinations follow the same rules independently of the reagents and they have distinctive patterns in CV. We will discuss some of the most important mechanisms in organometallic electrochemistry.

The simplest reaction studied by electrochemical methods is a one-electron step (E reaction)

$$O + e^- \rightarrow R \qquad (2)$$

When ET between an electrode and an electroactive
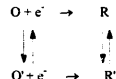
Scheme 1.

species proceeds at the thermodynamic potential of the electroactive species the reaction is called electrochemically reversible, Nernstian or simply fast. When the potential required to transfer the electron between the electrode and the electroactive species is much larger than the thermodynamic potential of the electroactive species the electrochemical reaction is then called slow or irreversible. The difference between the required electrode potential and the thermodynamic potential of the electroactive species is termed overpotential.

Reactions that appear to be simple E reactions may involve significant structural changes, so that chemical steps need to be included. Thus, Eq. (2) may be split into a square scheme with horizontal E-steps and vertical C-steps (Scheme 1).

When the chemical steps are in equilibrium in the time scale of the experiment, the system behaves as a single ET reaction of equilibrated O/O' to produce R/R'. Laviron and co-workers have provided a comprehensive analysis of the schemes of squares for different cases [57–67] [68,69]. Nowadays, with the availability of spectroelectrochemical techniques, it is possible to observe in situ the structural changes produced by reactions at the electrode surface [11]. Meanwhile, ultrafast CV allows us to work at time scales never achieved before by electrochemical techniques.

One of the most common mechanisms found in organometallic electrochemistry is ECE. This is the type of mechanism involved in electrochemically initiated ET chain catalysis (ETC), which has become an important method for the synthesis of organometallic compounds.

3.1. ECE scheme

A generalized sequence of ECE reactions is given by Scheme 2. The ECE scheme involves many possible variations. For example, the shape of the cyclic voltammogram depends on the reversibility of the different steps and the relative E^0 values of the different couples involved. The theory for ECE reactions is well understood [70–74], including preparative-scale aspects [75–81]. We discuss here only the most common cases

$$O + e^- \rightarrow R$$
$$R \rightarrow R'$$
$$R' + e^- \rightarrow R''$$
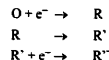
Scheme 2.

found in organometallic electrochemistry and how the techniques discussed before can help us to obtain a better insight into the nuances of the different mechanisms.
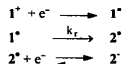
3.1.1. ECE-DISP scheme

In the general scheme for ECE reactions R' is formed in solution and reduced at the electrode surface. A common behavior observed in organometallic electrochemistry [82-85] is that R' is reduced by R before it can reach the electrode surface. The reaction is formally a disproportionation in that R and R' are at the same oxidation state. We have to add to Scheme 2 the following equation:

$$R + R' \rightarrow O + R'^- \tag{3}$$

The scheme of reactions depicted by Scheme 2 and Eq. (3) combines the ECE mechanism with a disproportionation reaction (ECE-DISP). It is important to point out that R'^- is formed both at the electrode surface and in solution. The analysis of this mechanism is complicated and requires digital simulation.

An interesting example is the work of Kuchynka and Kochi [85]. They studied the reduction of *trans*-$Mn(CO)_2(\eta^2\text{-dppe})_2^+$ (1^+) in tetrahydrofuran. 1^+ (closed) is reduced in an overall two-electron process to produce the anion 2^- (open) in which one end of a dppe ligand has been displaced, forming a ring-opened

A. Experimental   B. Simulated (ECE)

Fig. 3. (A) Initial negative scan (four-cycle) cyclic voltammograms of 5 mM 1^+ at 500 mV s^{-1}. (B) Computer-simulated CV according to ECE mechanism in Scheme 3. Reprinted from Ref. [85] © American Chemical Society.

Scheme 3.

structure. An experimental multicycle voltammogram of 5 mM 1^+ at 500 mV s^{-1} is shown in Fig. 3(A).
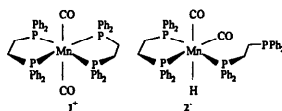
The ECE sequence represented in Scheme 3 is the most economical pathway for the reduction of the cationic $Mn(CO)2(dppe)_2^+$ to the anion 2^-. Fig. 3 shows the computer simulations (Fig. 3(B)) of the experimental cyclic voltammograms (Fig. 3(A)) over a sequence of four repetitive cycles considering Scheme 3. The CV simulations were carried out by using Feldberg's finite difference method [29]. Although the general features of the computer-simulated cyclic voltammograms in Fig. 3 resembled the experimental ones, the authors pointed out three important discrepancies:

(a) a pair of isopotential points (IPP) was observed in the simulated CV. However, they occurred at the same potential, which was not the situation in the experimental CV;

(b) no curve crossing was brought out in the simulated cyclic voltammograms;

(c) no cathodic peak current for the reduction of 1^+ on the fourth cycle was substantially larger than that observed experimentally.

These discrepancies pointed toward the necessity of including an additional factor that would reduce the concentration of 1^+. A disproportion process between 1^+ and its reduced product 2^- that gave rise to the pair of radicals 1^- and 2^- could produce this effect, i.e.

$$1^+ + 2^- \rightarrow 1^- (19e^-) + 2^- (17e^-) \tag{4}$$
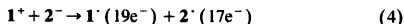
Owing to the rapid conversion of the 19e$^-$ radical to 2, this process was approximated as

$$1^+ + 2^- \rightarrow 2 2^- \tag{5}$$

Fig. 4 shows the computer-simulated voltammogram constructed from the ECE-DISP model based on Scheme 3 and Eq. (5). Excellent agreement with the experimental CV was obtained with the same electrochemical parameters employed in Fig. 3(B).

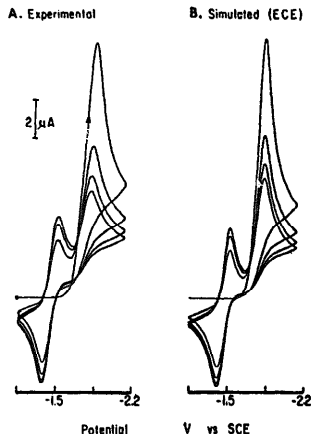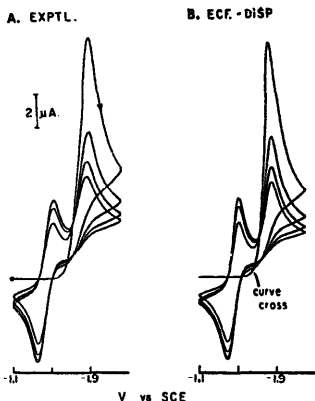The mathematical treatment of ECE schemes is very

Fig. 4. (A) Repetitive four-cycle CV of Mn(CO)$_2$(dppe)$_2^+$ as in Fig. 3(A). (B) Computer-simulated CV based on ECE–DISP mechanism with the inclusion of Eq. (5). Reprinted from Ref. [85] © American Chemical Society.
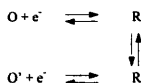

Fig. 5. Voltammograms of cis-W(CO)$_2$(dppe)$_2$ (R) in 0.2 mM Bu$_4$NClO$_4$–dimethylformamide at a platinum disk microelectrode (radius 62.5 μm). O' and R' designate the trans isomer. (a) 100 V s^{-1}. (b) 1000 V s^{-1}. Adapted from Ref. [86] © American Chemical Society.

complicated, and only in extreme cases are analytical solutions obtained. In most of the ECE reaction schemes, digital simulation techniques, combined with the data obtained by CV, are used to disclose the mechanism involved.

3.1.2. ECE—square scheme

This mechanism can be represented as a restricted square scheme (Scheme 4). In this case, R' is oxidized to O', rather than further reduced to R'$^-$ (Scheme 2). The main difference with the whole square scheme is that the species O and O' do not interconvert in the time scale of the experiment. The nature of the voltammetric response depends on the relative values of $E_{O/R}^0$ and $E_{O'/R'}^0$. Two situations may be considered, when R' is more difficult to oxidize than R ($E_{O'/R'}^0 - E_{O/R}^0 > 0$) and when R' is easier to oxidize than R ($E_{O'/R'}^0 - E_{O/R}^0 < 0$).

3.1.2.1. $E_{O'/R'}^0 - E_{O/R}^0 > 0$.
When ($E_{O'/R'}^0 - E_{O/R}^0 > 0$), the reduction of O proceeds by a simple EC reaction to give R'. In CV experiments O' is formed in the return scan.

A good example is the isomerization of cis-

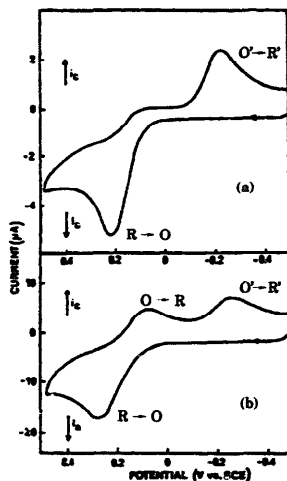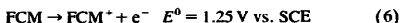W(CO)$_2$(dppe)$_2$ (R) [86]. Cyclic voltammograms for oxidation of R in dimethylformamide are shown in Fig. 5. In this case the cis form is favored in the neutral complex (reduced form) whereas trans predominates at equilibrium in the oxidized form (O'). Upon oxidation at +0.2 V, R forms short-lived O that rapidly isomerizes to the trans isomer (O'). Consequently, no peak for the reduction of O to R is detected on the reverse sweep at a scan rate of 100 V s^{-1} (Fig. 5(a)). Instead, the reverse sweep features a single prominent peak for reduction of O' to R'. At a scan rate of 1000 V s^{-1} a peak for the reduction of O is observed (Fig. 5(b)) since the time scale of the experiment does not allow the conversion of O to O'. Using ultrafast CV a complete analysis was achieved, including evaluation of the reversible potentials, equilibrium constants for the chemical steps, and rate constants for the chemical steps.

Another example involves the use of ESR in situ to study the mechanism of the isomerization of fac-[Mn(CO)$_3$Cl(dppm)] (dppm = bis(diphenylphosphino)methane) in acetonitrile [87,88] which can be analyzed by an EC mechanism:

$$FCM \rightarrow FCM^+ + e^- \quad E^0 = 1.25 \text{ V vs. SCE} \quad (6)$$

$$FCM^+ \rightarrow MCM^+ \quad (7)$$

Scheme 4.

$$
\begin{array}{ccc}
O + e^- & \rightleftharpoons & R \\
 & & \updownarrow \\
O' + e^- & \rightleftharpoons & R'
\end{array}
$$

with further electrochemical detection of MCM^+ by reduction in the reverse scan at 0.83 V:

$$MCM^+ + e^- \rightarrow MCM \qquad (8)$$

where FCM is *fac*-tricarbonylchloro[bis(diphenylphosphino)methane] manganese(I) and MCM is the mer isomer. Molecular evidence of the reaction product was found by ESR experiments with a TE_{102} cavity and a channel cell; the electrolysis of FCM at 1.30 V under transport limiting conditions produced an ESR spectrum of MCM^+ cation.

Under light irradiation ($\lambda = 390$ nm) a new oxidation wave was observed at 0.85 V with increase also of the anodic current due to oxidation of *fac*-$Mn(CO)_3Cl(dppm)$ at 1.25 V. The new redox system MCM^+/MCM could be seen in further cycles at 0.83–0.85 V both in anodic and cathodic peaks. The photochemical–electrochemical reaction sequence is

$$FCM + h\nu \rightarrow MCM \qquad (9)$$

$$MCM \rightarrow MCM^+ + e^- \quad E^0 = 0.83\,V \qquad (10)$$
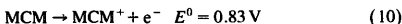
The action spectra (plots of transport-limited photocurrent against excitation wavelength) at 0.85 V and 1.25 V were identical in shape, suggesting that they arose from the excitation of FCM by comparison with the UV–visible absorption spectrum of FCM and MCM with $\lambda_{max} = 390$ nm (fig. 4 in Ref. [87]).

In situ electrochemical ESR at 0.90 V with simultaneous irradiation at $\lambda = 390$ nm of FCM produced a six-line spectrum of Mn(II) identical to the spectrum of the electrochemical oxidation product of FCM (reactions in Eqs. (6) and (7)) and provided evidence for the formation of MCM^+ cation. However, no ESR spectrum was obtained in the dark. At 1.30 V the same ESR spectrum as for MCM^+ was observed in the dark and under irradiation, with a larger signal in the latter case.

Some evidence for the disproportionation step

$$2FCM^+ \rightarrow FCM + FCM^{2+} \qquad (11)$$
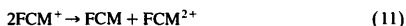
was suggested from the action spectrum at 1.25 V where FCM is destroyed electrochemically while at the same time this is the light absorbing species.

The above example shows that reactive intermediates can be obtained both photochemically and electrochemically. By combination of spectroscopy, photochemistry and electrochemistry, detailed mechanistic information can be gained.

Furthermore, photocurrent vs. flow rate data fits for the OTTLE channel electrode flow cell [89] proved to be diagnostic of a photo-CE mechanism by careful analysis of the spatial and time distributions of the reaction intermediates.

Other examples of this type of mechanism are given by the groups of Bond [21] and Geiger [90,91]. Bond et al. were able to resolve the mechanism involved in the isomerization of $[Cr(CO)_2(dppe)_2]^+$ by using micro-electrode and rotating-disk techniques in several solvents including toluene and benzene. Geiger and coworkers studied the isomerization of a cobalt complex: $CpCo(1,5\text{-}C_8H_8)$. They found that one-electron reduction of this complex produced an anion radical with a different isomeric make-up, but still containing a di-olefin-bound C_8H_8 ring, $[CpCo(1,3\text{-}C_8H_8)]^-$. Using ultrafast CV and spectroscopic techniques, such as ESR and ^1H NMR, they were able to elucidate the different structures.

3.1.2.2. ETC ($E_{O'/R'}^0 - E_{O/R}^0 < 0$). In this case the reaction between the reactant O and R' needs to be added to Scheme 4:

$$O + R' \rightarrow R + O' \qquad (12)$$

At the potential where O is reduced, the R' formed from R can be oxidized to O', either at the electrode surface or in solution by O. Thus, the conversion of O to O' is catalyzed by ET. Because of the combination of the R to R' step and Eq. (12) constitutes a chain reaction, the process is termed ETC. ETC (also named electrocatalysis) belongs to the family of chain reactions [92,93] where the electron is the catalyst. As electrons are involved in this type of reaction, electrochemical methods are well suited for mechanistic studies and bulk electrolysis is a convenient method for the synthesis of new organometallic compounds. Feldberg and Jeftic [94] were the first to study this type of reaction using electrochemical methods.

In ETC, the overall reaction usually proceeds without net redox change. Thus for an isomerization reaction we have

$$O \rightleftarrows O' \qquad (13)$$
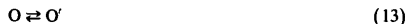
Meanwhile, in the case of ligand exchange:

$$ML_n + L' \rightleftarrows ML_{n-1}L' + L \qquad (14)$$

CV provides a unique insight into the mechanism of electrocatalysis. Fig. 6 shows how the addition of triphenylephosphine (L' in Eq. (14)) leads to a drastic alteration of the reversible CV of $\eta^5\text{-MeCpMn(CO)}_2L$ (R) (Fig. 6(a)), where L in this case is acetonitrile (NCMe) [95]. The reactant wave (R) in Fig. 6(b) becomes irreversible, as indicated by the absence of the coupled cathodic wave. Furthermore, the anodic peak current for R decreases in magnitude in proportion to the concentration of triphenylphosphine (PPh_3), and the diffusion current falls to near zero. This behavior requires that R be removed from the vicinity of the electrode by some alternative process that does not require a net flow of current. Such a process simultaneously leads to the substitution product (P), which is clearly in evidence in Fig. 6(b) and Fig. 6(c), by its reversible CV wave at $E^0 = 0.55$ V. The anodic electrode process leads to the depletion of R and results in the concomitant formation of P.
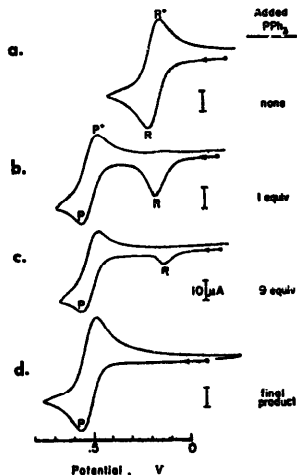
Fig. 6. Effect of added PPh$_3$ on the reversible CV of MnX(NCMe), $(x = \eta^5\text{-MeCp(CO)}_2)$ R, at a scan rate of 200mV s^{-1}. The CV waves of R and MnX(PPh$_3$), P, are indicated for solutions containing (a) 0, (b) 1 and (c) 9equiv. of PPh$_3$. (d) CV of pure P under the same conditions. Adapted from Ref. [95] © American Chemical Society.

When one of the isomers is more difficult to reduce than the other, ETC is a convenient way to produce isomerization (Scheme 4). As an example, Mevs and Geiger [96] in their study of a trirhodium cluster (3 and 4; Cp = η^5-C$_5$H$_5$), one of the two forms, 4, is the more stable. Both isomers are reduced to stable anions that do not isomerize ($E_{3/3}^{0-} = -1.22$ V vs. SCE, $E_{4/4}^{0-} = -1.01$ V vs. SCE) but oxidation of solutions of 3 leads to rapid ETC isomerization to 4. The process is so rapid that absolutely no oxidation peak for 3 could be detected even at a scan rate of 100V s^{-1}. The authors conclude that the rate constant for the isomerization of 3^+ to 4^+ must exceed 10^{5}s^{-1}. As no oxidation peak could be observed, an indirect method was used to estimate the potential for Eq. (15):

$$3^+ + e^- \rightarrow 3 \tag{15}$$

3   4
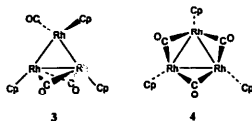
Voltammetric reduction of a solution of 3 reveals a single peak when the initial potential is about 0.2 V vs. SCE (Fig. 7, top). However, when the initial potential is more positive, the voltammograms reveal a peak for reduction of 4 (Fig. 7, middle and bottom). Thus the reductive voltammograms provide a means of monitoring the oxidative ETC isomerization. By using a fast sweep rate that 'freezes' the reaction-diffusion layer, the cathodic peak height for 4 was measured after holding the potential for 15s at a series of initial potentials. The peak current of the isomer reduction increases sigmoidally as a function of the initial potential. From the midpoint of this sigmoidal curve a formal potential value for the 3$^+$/3 couple was estimated to be 0.25 V. Other examples of ET-catalyzed isomerization can be found in the literature [97–104].

Ligand exchange and decomposition of organometallic compounds catalyzed by ET have been studied in several systems. A good example is the reactivity gained by iron complexes when the iron nucleus is reduced to Fe(I). Moinet et al. [105] studied the electroreduction of η^5-cyclopentadienyl iron η^6-arene cations which produces radicals of the same formula. The behavior of these radicals depends on the nature of the substituents on the rings and on the medium. The studies were carried out using conventional CV and polarography. Decomposition, dimerization and catalysis were found as possible reactions. They found that the cathodic reduction of the complex in 95% ethanol (Hg pool, 0.1 M LiOH) provides quantitatively Fe^{2+}, cyclopentadiene and benzene. Later, Darchen [106] studied the reduction of the same compound and the coordination
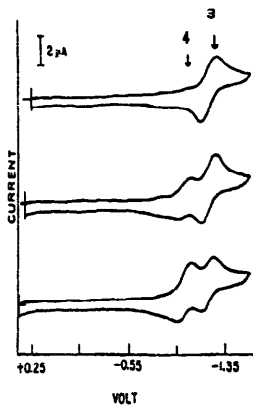

Fig. 7. Cyclic voltammograms of compound 3 in THF as a function of the initial potential: 0.25 V (top), 0.30 V (middle), 0.35 V (bottom). Adapted from Ref. [96] © American Chemical Society.

of the radical formed with the solvent molecules. The increasing stability of η^5-cyclopentadienyl Fe(I) η^6-arene follows the order of solvent used: acetonitrile or pyridine < dimethylformamide < acetone or methylene chloride. In acetonitrile, the fast replacement of the arene by donor ligands occurs via a postulated intermediate η^5-C$_5$H$_5$Fe(I)(CH$_3$CN). Without donor ligands, decomposition leads to the corresponding ferrocenes.
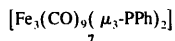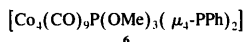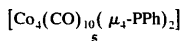
Rieger and co-workers [107] studied electron-induced substitution in Fe(CO)$_5$ initiated by reduction in the presence of phosphites or phosphines. The reduction of this compound produces a dimer, Fe$_2$(CO)$_8^{2-}$, presumably with Fe(CO)$_4^{\cdot-}$ and Fe(CO)$_4^-$ as short-lived intermediates. In this case the action of the nucleophile is to trap Fe(CO)$_4^{\cdot-}$. Radical dimerization of Fe(CO)$_4^{\cdot-}$ competes very effectively and only 10% substitution is obtained.

An important body of work was done on ETC reactions of carbonyl clusters. The electrocatalytic substitution of one or several carbonyl ligands by P or As donors or by isonitriles in transition-metal carbonyl clusters is induced by monoelectronic reductants. In this case, electrochemical techniques are well suited since the electrode potential for the reaction can be established to produce a selective substitution of ligands. Rieger and co-workers [107] showed that CO ligands can be readily replaced by phosphite or phosphine ligands in clusters of the type [XCCo$_3$(CO)$_9$] (X = Ph,Cl) by a cathodic current. D.C. polarographic and cyclic voltammetric studies show that the reduction current wave of the initial compound decreases in the presence of the P-ligand as the expected wave for the substitution product appears. A similar behavior was found with the binuclear compound [(PhCCPh)Co$_2$(CO)$_6$]. It was proposed that radical anions of the bi- and trinuclear cobalt complexes have their extra electron in metal–metal antibonding orbitals, which leads to Co–Co bond cleavage, as depicted in Scheme 5. In agreement with the proposed mechanism, Rieger and co-workers [108] observed that the anodic–cathodic CV peak current ratio for the primary electrode process is not affected by the presence of Lewis bases or CO. Thus, the rate-limiting step involves a reaction of this radical anion with a species that reacts rapidly with the Lewis base, but the rate-limiting step does not involve the Lewis base itself.

Kochi and co-workers have examined the sequential

Scheme 6.
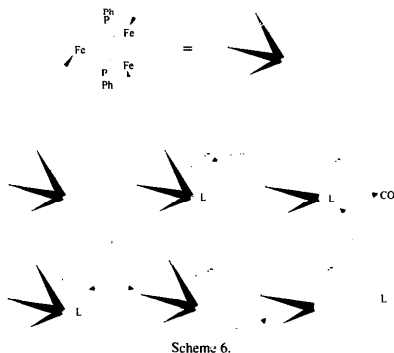
replacement of CO ligands in the phosphanediyl-capped clusters (5–7) by P-donor ligands, essentially using a cathodic current [109–111].

$$\left[\underset{\mathbf{5}}{Co_4(CO)_{10}} (\mu_4\text{-PPh})_2 \right]$$

$$\left[\underset{\mathbf{6}}{Co_4(CO)_9 P(OMe)_3} (\mu_4\text{-PPh})_2 \right]$$

$$\left[\underset{\mathbf{7}}{Fe_3(CO)_9} (\mu_3\text{-PPh})_2 \right]$$

In Co clusters [109,110], coulombic efficiencies were between 4 and 11, because radical anionic intermediates tend to decompose at competitive rates. The lifetimes of the primary radical anions are independent of the P donor concentrations, indicating that the rate-limiting step does not involve the nucleophilic attack on the primary radical anion; rather, it involves the formation of another intermediate that reacts with the P donor molecule.

The studies on the electrocatalysis of **7** [111] demonstrated the need for generating a reactive '17e$^-$ center' by cleavage of one cluster edge. Transient ESR studies combined with the analysis of the cyclic voltammograms allow the authors to propose the following mechanism (Scheme 6): the opening of an Fe–P bond, the reaction of PEt$_3$ or P(OMe)$_3$ with the temporary open cluster anion, and the closure of the phosphine-substituted open cluster anion to the substituted closed one. The experimental results indicate that Fe–P cleavage is preferred over Fe–Fe cleavage and highlights the crucial role of the phosphanediyl cap.

In a later section we will discuss the use of electrocatalysis in the synthesis of organometallic compounds and its comparison with the thermal excitation mechanism.
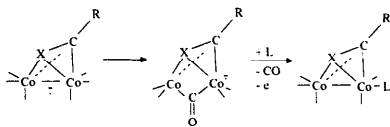
Scheme 5.

3.2. ECEC mechanism

Using conventional CV, Bond and co-workers [112] and Roth and Kaim [113] studied the isomerization of different organometallic compounds that involves the ECEC mechanism.

Roth and Kaim studied the ET isomerization $\eta^2(C=C) \rightarrow \eta^1(N)$ of the tetracyanoethylene complex $(C_6N_4)W(CO)_5^{0/-}$. They concluded that conventional CV is not enough to disclose unmistakably the organometallic molecular process involved. Experiments at higher scan rates and the use of several spectroscopic techniques are necessary. Meanwhile, Bond and co-workers studied the electrochemical behavior of cationic carbonyl hydride complexes of Group VI transition metals. They established that the electrochemical experiments carried out were not able to distinguish between a number of possible mechanisms.

This work, made by leading groups in organometallic electrochemistry, shows the need for more sophisticated techniques to elucidate a more complex mechanism.

3.3. Electrochemistry as a tool for the mechanistic study of heterogeneous phase reactions
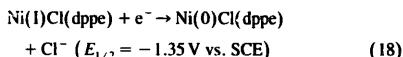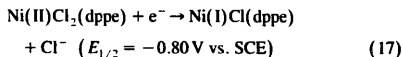
The synthesis of symmetrical or asymmetrical biaryls involves the use of catalytic amounts of zero-valent transition metal. Several attempts to elucidate the role of the zero-valent transition metal catalyst have been made. Among them, Amatore and Jutand [114–116] have used the conceptual analogies between electrochemically initiated homogeneous reactions and their equivalents taking place at the surface of metal particles. The advantage of this approach is that electrochemistry can provide kinetic information about the region where the reaction develops. This region is close to the metal surface for a heterogeneous reaction. In a reaction initiated electrochemically, this region is the electrode surface. In both cases a diffusion-reaction layer is formed, but electrochemical techniques have a better control of the reaction conditions.

The investigations of the rates and mechanism of homocoupling and carboxylation of aryl halides catalyzed by nickel complexes were done by an electrochemical approach [114]. The same methodology was extended to palladium complexes [115]. As an example, we discuss here the nickel catalysis of bromobenzene homocoupling to biphenyl [116].
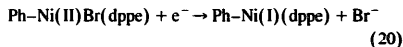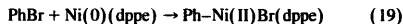
When bromobenzene is electrolyzed in the presence of $NiCl_2$(dppe) in a molar ratio 9:1, biphenyl is obtained quantitatively:

$$2PhBr + 2e^- \xrightarrow{10\% NiCl_2(dppe)} Ph-Ph + 2Br^-$$

$$E \leq -2\,V \text{ vs. SCE} \tag{16}$$
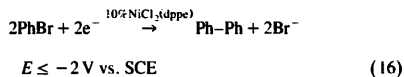
Using electrochemical techniques, the authors observed the existence of a threshold potential, a fact difficult to reveal when a metal is used as the reductant. They also observed that when electrolysis is performed at potentials less negative than $-2\,V$ vs. SCE, no biphenyl is obtained, but two faradays per mole of nickel complex are used and one equivalent of bromobenzene is consumed to yield a phenylnickel(II) derivative, Ph–Ni(II)(dppe)Br. Voltage sweep voltammetry reduction of $NiCl_2$(dppe), without PhBr, occurs in two one-electron waves:

$$Ni(II)Cl_2(dppe) + e^- \rightarrow Ni(I)Cl(dppe)$$
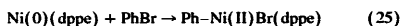$$+ Cl^- \;(E_{1/2} = -0.80\,V \text{ vs. SCE}) \tag{17}$$

$$Ni(I)Cl(dppe) + e^- \rightarrow Ni(0)Cl(dppe)$$
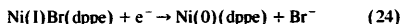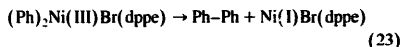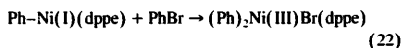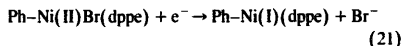$$+ Cl^- \;(E_{1/2} = -1.35\,V \text{ vs. SCE}) \tag{18}$$

In the presence of bromobenzene, the development of a third wave is observed ($E_{1/2} \approx -1.3\,V$ vs. SCE), which can be shown independently to correspond to the one-electron reduction of a phenylnickel(II) complex formed by oxidative addition of PhBr to the zero valent nickel electrogenerated in the second wave (Eq. (18)). Eq. (19) and (20) depict the reactions involved.

$$PhBr + Ni(0)(dppe) \rightarrow Ph-Ni(II)Br(dppe) \tag{19}$$

$$Ph-Ni(II)Br(dppe) + e^- \rightarrow Ph-Ni(I)(dppe) + Br^- \tag{20}$$

From fast CV the rate of the oxidative addition in Eq. (19) has been determined to be $10^5\,M^{-1}\,s^{-1}$; this is several orders of magnitude greater than those corresponding to the chemically saturated zero-valent nickel complexes [117,118].

The reduction of PhNi(II)Br(dppe) is required to initiate the process, since in preparative electrolytic experiments the potential must be located more cathodic than in Eq. (20). Amatore and Jutand demonstrated that the following mechanism is involved:

$$Ph-Ni(II)Br(dppe) + e^- \rightarrow Ph-Ni(I)(dppe) + Br^- \tag{21}$$

$$Ph-Ni(I)(dppe) + PhBr \rightarrow (Ph)_2Ni(III)Br(dppe) \tag{22}$$

$$(Ph)_2Ni(III)Br(dppe) \rightarrow Ph-Ph + Ni(I)Br(dppe) \tag{23}$$

$$Ni(I)Br(dppe) + e^- \rightarrow Ni(0)(dppe) + Br^- \tag{24}$$

$$Ni(0)(dppe) + PhBr \rightarrow Ph-Ni(II)Br(dppe) \tag{25}$$

They observed that the reduction of Ni(I)Br(dppe) is largely exergonic at the electrode potential used in preparative experiments ($E < -2\,V$ vs. SCE); similarly, within the time scale of steady-state voltammetry,

the oxidative addition step in Eq. (25) is sufficiently fast not to be involved in the kinetic control of the overall sequence. The rate of this sequence of reactions is then controlled by the slower step between Eqs. (22) and (23). At low PhBr concentrations oxidative addition of bromobenzene concentrations to the phenylnickel(I) derivative forces the overall rate to be first order in nickel and first order in PhBr. In this case, the current will depend on the square root of PhBr concentration. At larger concentrations of bromobenzene the reductive elimination of biphenyl from nickel(III) species in Eq. (23) becomes the rate-determining step and the current has no dependence on the bromobenzene concentration.

The authors pointed out that the electrode–solution interface is structured in a fashion similar to a particle–solution interface. However, now all kinetic data are sampled at the electrode surface and depend on the exact concentration profiles in the close vicinity of the electrode surface. Since diffusion of molecules at an electrode surface is easily modeled, one can derive the theoretical rate law corresponding to a given sequence of reactions and compare its predictions with the actual experimental data.

3.4. Thermodynamics

In this section, we plan to introduce the methodology developed by Parker and co-workers to obtain thermodynamic data meaningful for reactions in solution. Later, we will discuss the use of microelectrodes and ultrafast CV to determine electrode potentials for short-lived species.

Wayner and Parker pointed out that thermochemical cycles incorporating electrode potentials provide a means of obtaining thermodynamic data for reactions in solution that are either difficult or impossible to obtain directly [119]. The rigorous application of thermochemical cycles requires reversible electrode potentials. These are thermodynamically significant quantities defined as the electrode potential at which equal concentrations of the reduced (R) and oxidized (O) forms of the redox couple exist in equilibrium (Eq. (2)).

In order that the measurements actually reflect the reversible potential, equilibrium must be attained. This implies that both reduced (R) and oxidized (O) forms must be long-lived and that the charge transfer must be rapid relative to the time scale of the measurement. The latter criterion is often referred to as Nernstian or reversible.

The two criteria stated above for the measurement of reversible electrode potentials are often in conflict. For instance, if it is necessary to use a very rapid technique (to detect the existence of both R and O) the charge transfer may not appear as Nernstian. On the other hand, at slow scan rates follow-up reactions can occur, hence the concentrations of the electroactive species not
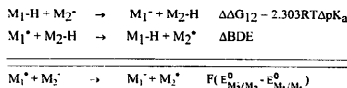
only depend on the electrode potential but also on the kinetic constant of the following reaction. This translates into a shift of the electrode potential giving an error in the thermochemical quantity derived from the irreversible peak potential.

CV is a simple and powerful method to determine if an electroactive species behaves as Nernstian from the difference between anodic and cathodic potential peaks ($\Delta E_p = 60$ mV for a one-electron reversible couple). A non-Nernstian behavior or a following reaction can affect the value of ΔE_p. Two approaches can be adopted to minimize the error due to ΔE_p. One of them is to estimate the rate constants of the homogeneous follow-up reaction. This can be done by recording voltammograms at different scan rates and concentrations, since the different mechanisms (EC, ECE, etc.) follow different expressions that depend on the scan rate and the concentration of the electroactive species [14]. The second approach is to increase the voltage scan rate in order to diminish the effect of the kinetic step on the peak potential. However, the second method requires the use of microelectrodes and more sophisticated instrumentation.
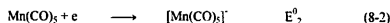
In the study of organometallic compounds the knowledge of the bond dissociation energy (BDE) of metal–hydrogen, metal–metal and metal–carbon is essential to distinguish between mechanistic possibilities. Tilset and Parker pointed out that thermochemical data for the homolytic metal hydrogen (M–H) BDE of organotransition-metal hydrides are scarce and that those available were derived from metal–metal (M–M) BDE estimates that vary over wide ranges [120]. These authors estimated M–H BDEs by using a thermodynamic cycle that requires the knowledge of the M–H Brønstead acidity and the reversible oxidation potential of the corresponding M$^-$ anion. They made use of the isodesmic reactions (reactions where the total number of bonds remains constant) to construct a relationship. Having access to experimental values mentioned before and the value of BDE for M$_1$–H, it is possible to determine the BDE value for any other compound, M$_2$–H, as illustrated in Scheme 7 [121].

Using this approach Wayne an Parker [119] and Tilset and co-workers [120–123] have accumulated an important body of thermochemical data for M–H and M–C BDEs for organometallic compounds .

Pugh and Meyer [43] used ultrafast CV combined with a redox equilibration technique to determine free

$$M_1\text{-H} + M_2^{\cdot-} \quad \rightarrow \quad M_1^{\cdot-} + M_2\text{-H} \quad \Delta\Delta G_{12} - 2.303RT\Delta pK_a$$

$$M_1^{\cdot+} + M_2\text{-H} \quad \rightarrow \quad M_1\text{-H} + M_2^{\cdot} \quad \Delta BDE$$

$$M_1^{\cdot+} + M_2^{\cdot-} \quad \rightarrow \quad M_1^{\cdot-} + M_2^{\cdot} \quad F(E^0_{M_2/M_2} - E^0_{M_1/M_1})$$

Scheme 7.

$$Mn_2(CO)_{10} + 2e \quad \longrightarrow \quad 2\,[Mn(CO)_5]^- \qquad E^0_1 \qquad (8\text{-}1)$$

$$Mn(CO)_5 + e \quad \longrightarrow \quad [Mn(CO)_5]^- \qquad E^0_2 \qquad (8\text{-}2)$$

$$Mn_2(CO)_{10} \quad \longrightarrow \quad 2\,Mn(CO)_5 \quad \Delta G^0 = -2F(E^0_1 - E^0_2) \quad (8\text{-}3)$$

Scheme 8.

energy changes in metal–metal bond homolytic dissociation. As an example we use the determination made for $Mn_2(CO)_{10}$ (Scheme 8).

The irreversibility of the two-electron reductions or oxidations, as in reaction (8-1) of Scheme 8, precluded the measurements of E^0 values by CV. The potentials of these couples were measured by redox equilibration. A couple of known potential was mixed with $Mn_2(CO)_{10}$, both of them in a known concentration. Changes in concentration were followed by changes in IR band intensities characteristic of the reagents present in solution. When the system reached equilibrium, the final concentrations were determined; therefore, the equilibrium constant could be established. From the known redox potential of the auxiliary couple and the equilibrium constant, the redox potential of the two-electron couple of reaction (8-1) in Scheme 8 was determined.

In order to determine the redox potential of the couple depicted in reaction (8-2) in Scheme 8, $[Mn(CO)_5]^-$ was generated. At very fast scan rates $(5000\ V\,s^{-1})$ the oxidation of $[Mn(CO)_5]^-$ to $[Mn(CO)_5]$ is reversible because the reduction of $[Mn(CO)_5]$ to $[Mn(CO)_5]^-$ is faster than the dimerization to give $Mn_2(CO)_{10}$. From the redox potential of the couples $Mn_2(CO)_{10}/[Mn(CO)_5]^-$ and $[Mn(CO)_5]^-/[Mn(CO)_5]$ the free energy change of metal–metal bond dissociation is established, as shown in Scheme 8.

4. Electrosynthesis

In recent years, there has been a growing concern in the use of raw materials and energy production compatible with a clean environment. In this context, electrosynthesis represents a convenient method when electrons are involved as reactants or catalysts, since it is more selective and energetically more efficient.

Electrode reactions provide fine control of reaction free energy. Both the equilibrium position and the kinetics can be altered by approximately 10^{16}-fold and 10^9-fold respectively when the electrode potential is changed by 1 V [124].

Reactions at electrodes provide milder conditions than thermal routes for the production of highly reactive intermediates. For instance, thermal reactions offer conditions of lower selectivity and yield than ETC (vide infra).

Electrochemistry in organometallic synthesis is used in different ways. It can be used to produce an in situ reactant or catalyst by electrolysis using inert electrodes, as starting material (either as sacrificial anode or cathode), and as a source or sink of electrons to initiate a reaction in electrocatalysis.

4.1. Sacrificial electrodes

The use of sacrificial electrodes in the synthesis of organometallic compounds is a well established method [6]. Recent reviews dealing with the electrochemical dissolution of metal electrodes were written by Tuck [125], Grobe [126] and Vechhio-Sadus [12].

Tuck and co-workers [127–131] have synthesized a series of organometallic halides using titanium, zirconium, hafnium [127], zinc, cadmium [128,129], magnesium [130], indium [131] and other metals [125]. The metal is used as anode in a cell containing a solution of organic halide RX in acetonitrile or methanol. The mechanism proposed for titanium, zirconium and hafnium involves the cathodic reduction of an organic halide followed by the migration of the halide ion to the anode where MX is formed. Then, this species undergoes a variety of oxidative insertion reactions yielding R_2MX_2 species stabilized in situ as adducts with neutral donors. In the case of magnesium, the adducts (e.g. $RMgX\cdot bipy$, where bipy is bipyridine) and salts $[R_4N(R'MgX_2MeCN)]$ do not have typical Grignard reagent chemistry. For indium, low oxidation states can be obtained by this technique.

Banait and Pahil [132,133] synthesized organocopper(II) complexes with stoichiometry $Cu(CR)_2$ and $Cu(CR_2)$. Using a Cu anode, they carried out electrolysis of organic precursors with one or two functional groups that have withdrawing properties, such as nitromethane, nitroethane, MeCN, malonitrile, diethylmalonate and cyanoacetamide. These compounds have abstractable protons yielding compounds with general formula $Cu(CR)_2$ for those with one functional group or $Cu(CR_2)$ for those with two functional groups.

Successful preparations of a range of metallocenes and methylated metallocenes have been achieved directly from the metal (Fe, Co, Ni) and cyclopentadiene in DME–acetonitrile, THF–acetonitrile or acetonitrile [134–136]. The use of electrolysis is far superior to the conventional use of the alkali salt of the diene. Complexes are isolated as products of excellent purity and crystallinity.

4.2. Electrocatalysis

In Section 3.1.2.2 we discussed the mechanism of ETC and the use of electrochemical techniques for mechanistic studies. Chain initiation can be carried out chemically or at an electrode surface. For chemical

initiation we have to look for a compound with the right potential and suitable physical properties. Using an electrochemical method the rate of reactions and number of electrons transferred can be adjusted by the electrode potential leading to selective transformations. One-electron transfer steps with formation of ion-radicals and highly reactive intermediates can be achieved by tuning the electrode potential. Also, the same system can be used for different reactions initiated at different potentials which, for instance, allows the selective substitution of ligands in clusters (vide infra).

All types of reactions have been electrocatalyzed [137,138] including ligand exchange, insertion, extrusion and isomerization. The ligand-exchange reaction, however, has been by far the most studied [139,140]. The advantage of using these reactions in synthesis is the generation of $17e^-/19e^-$ species that produces a very fast associative ligand exchange (Eq. (26)) and the ability of transition metal species to undergo the redox reactions required in the whole cycle.

$$ML_n(17e^-) + L' \rightleftharpoons [ML_nL']^{2+} (19e^-)$$
$$\rightleftharpoons ML_{n-1}L'(17e^-) + L \qquad (26)$$
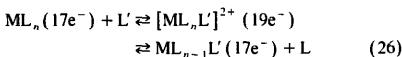
If an exergonic reaction is too slow, electrocatalysis can be an efficient means to overcome the kinetic problem. The reaction can be initiated by using the electrode as a source of electrons (reductive initiation, Scheme 9) or holes (oxidative initiation, Scheme 10).

There are two propagation steps in the mechanisms shown in Schemes 9 and 10, one of them must provide the driving force for the cycle. Even though the overall free energy of the reaction does not depend on the pathway, the mode of initiation (oxidative or reductive) is a key factor in the reaction rates. If nothing is known about the reversibility of the ligand exchange step, the driving force needed may be obtained from the ET propagation step (Eq. (27)) since the Marcus theory establishes that an exergonic ET is fast.

$$(ML_{n-1}L')^+/(ML_{n-1}L')^- + ML_n$$
$$\rightarrow ML_{n-1}L' + (ML_n)^+/(ML_n)^- \qquad (27)$$
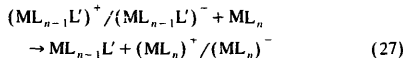
This means that, if $ML_{n-1}L'$ is easier to oxidize than ML_n ($E^0_{ML_{n-1}L'} < E^0_{ML_n}$), then it is possible to obtain a favorable driving force in the ET propagation by choosing reductive initiation. On the other hand, if $ML_{n-1}L'$ is more difficult to oxidize than ML_n ($E^0_{ML_n} < E^0_{ML_{n-1}L'}$)
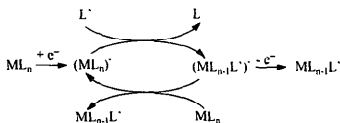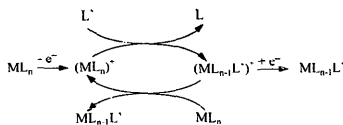

Scheme 9.

Scheme 10.

it is possible to gain the driving force in the ET propagation step by choosing oxidative initiation. The efficiency of the process is measured by the relation of the moles of starting material consumed divided by the faradays of charge passed through the solution; this relation is called coulombic efficiency.

Kochi and co-workers studied the ligand substitution of metal carbonyls (Eq. (28)) [95,141]. They studied ligand exchange electrocatalysis in carbonylmanganese derivatives, η^5-MeCpMn(CO)$_2$L, hereafter MnXL, using oxidative initiation [95].

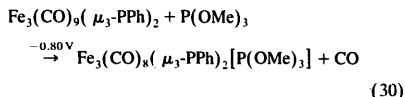$$MnXL + L' \rightarrow MnXL' + L \qquad (28)$$

Generally, the ligand substitution was carried out in acetonitrile (containing tetraethylammonium perchlorate as supporting electrolyte) using a set of platinum electrodes [95]. The electrolysis was generally carried out at constant current. Working in this way, it is possible to follow the ligand substitution by monitoring the electrode potential during the experiment. For example, for the ligand substitution of pyridine (py) by PPh$_3$, the starting potential at the platinum gauze anode (-0.13 V vs. saturated NaCl SCE) reflects the oxidation of MnX(py). The consumption of the reactant is accompanied by a gradual increase in the electrode potential until that time at which there is a sharp rise in the potential owing to the complete disappearance of MnX(py). The new plateau at 0.28 V is due to the oxidation of the product, MnX(PPh$_3$).

In most of the cases studied, the product (MnXL') is more difficult to oxidize than MnXL ($E^0_{MnXL'} > E^0_{MnXL}$), then electrochemical oxidative initiation is a well suited method for electrocatalysis. For these ligand substitutions, the reactions occur rapidly, quantitatively and with coulombic efficiencies over 1000 in some cases. However, when they considered the substitution of MnX(norbornene) by acetonitrile using oxidative initiation, only 15% yield of MnX(NCMe) was observed. Even though the overall ligand substitution process thermodynamically lies to the right (Eq. (29)), in this case $E^0_{MnX(norbornene)} > E^0_{MnX(NCMe)}$. The authors attributed the inefficiency of the process to the endergonicity of the ET step and the pathways available for the ready decomposition of MnX(NCMe)$^+$.

$$MnX(norbornene) + MeCN \rightarrow MnX(NCMe)$$
$$+ \text{norbornene} \qquad (29)$$
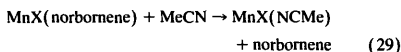
For $Fe_3(CO)_9(\mu_3\text{-PPh})$ (7), the exchange of one, two or three CO ligands by trimethylphosphite $[P(OMe)_3]$ ligands were obtained with coulombic efficiencies between 10 and 20 [111]. The authors found that each substitution product can be synthesized separately at room temperature in good yields by simply passing a small cathodic current (reductive initiation) through the solution of the cluster. The ligand substitution was carried out in either acetonitrile or tetrahydrofuran (THF) containing supporting electrolyte at a constant potential until 10–15% charge was consumed.

The first ligand substitution was carried out at a constant potential of -0.80 V vs. SCE (Eq. (30)).

$$Fe_3(CO)_9(\mu_3\text{-PPh})_2 + P(OMe)_3$$
$$\xrightarrow{-0.80\text{ V}} Fe_3(CO)_8(\mu_3\text{-PPh})_2[P(OMe)_3] + CO$$
(30)

The monophosphite product was isolated with a 65% yield; a similar result was obtained when triethylphosphine (PEt_3) was used under the same conditions. In the absence of cathodic current, the thermal substitution was not observed.

The bis-phosphite substitution product was obtained by passing a partial charge first at -0.80 V and then at -1.15 V. The yield was 63% for $P(OMe)_3$ and 66% when the added nucleophile was PEt_3.

The tris-phosphite substitution product was obtained directly from (7) working at a potential of -1.40 V by a procedure similar to that described above. However, the best result was obtained when the partially converted bis-phosphite was used.

Darchen and co-workers [142,143] studied the controlled substitution of CO by $P(OMe)_3$ in bimetallic iron complexes (8) using thermal activation or ET catalysis. The authors found that thermal substitution is not selective and leads to a mixture of mono- and di-substituted complexes 9 (62%) and 10 (29%). The monosubstituted product is regiospecific. Electrochemistry studies show an enhanced reactivity for the ligand substitution catalyzed by ET. Controlled potential electrolysis of 8 in the presence of $P(OMe)_3$ follows an ECE mechanism selectively affording monosubstituted products. The major complex 9 is accompanied by complex 11 in which $P(OMe)_3$ is bound to the same iron atom but occupies the axial position in contrast to complex 9 where $P(OMe)_3$ is equatorial. The authors also studied the isomerization of 11 to 9 by ET catalysis. They concluded that 11 is not the primary product of the thermal reaction but it is the kinetic product when the reaction is promoted by ET.

The efficiency and selectivity with which multiple processes, such as ligand substitution, be carried out under mild conditions in ET catalysis re an important advantage over the thermal activation echanism. This brings new opportunities for the synthesis of optically active clusters. The chirality results from a non-symmetric combination of ligands.
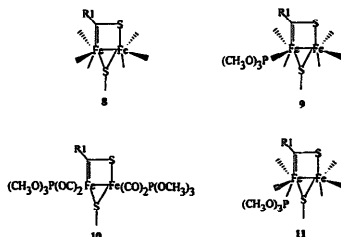
### 4.3. Electrochemical synthesis of catalysts

Périchon and co-workers [144] have reported an electrosynthesis of homoallyl alcohols and β-hydroxy esters in the presence of catalytic amounts of $NiBr_2(2,2'\text{-bi-pyridine})$ complex by mixed electrolysis of methallylchloride or methylchloroacetate with several carbonyl compounds, using a one-compartment cell equipped with a sacrificial zinc anode. Aromatic as well as aliphatic compounds give good yields of the corresponding alcohols, except for hindered ketones [145]. The proposed mechanism of the reaction involves the electrochemical reduction of the nickel bipyridine complex to produce a zero-valent nickel species that reacts with the allylic compound. The intermediate so produced reacts further with Zn(II) (originated by the oxidation of the zinc anode) and the starting ketone, producing a zinc alkoxide (Scheme 11). The nature of the nickel ligand as well as the anodic material are crucial factors, since replacing phosphine for bipyridine lowers the yield of alcohol significantly, the same as changing the zinc anode to Mn, Mg or Al. The method compares
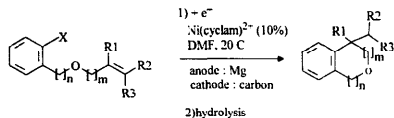

Scheme 11.
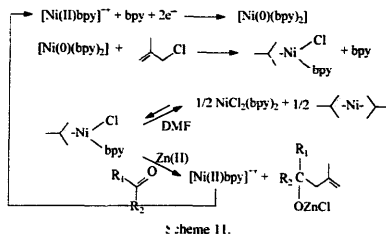
favorably with chemical procedures involving organometallics. the starting materials are allylic chlorides or acetates instead of bromides; the nickel complex is used in catalytic (instead of stoichiometric) amounts; as the coupling product is obtained in one step, the delicate preparation of the π-allyl nickel complex is avoided.

Another interesting example of this type of reaction is the electrochemical reductive cyclization of aromatic halides containing unsaturated ethers as ortho-substituents (Scheme 12) [146]. As with the previous case, a catalytic amount of Ni(cyclam)$^{2+}$ (cyclam = 1,4,8,11-tetraazacyclotetradecane) is used in conjunction with a magnesium anode. The product yields are good, and the electrochemical reaction has the advantage over chemical methods using tin hydride and Sn(II) species of not requiring reactive iodo derivatives, which can be replaced by chlorinated compounds. The electrochemical conditions used for this cyclization are very specific: a magnesium anode and a carbon fiber cathode are important for the production of cyclic compounds in good yields. The mechanism of the reaction involves a radical-type reactivity of the reduced aryl-halogen bond of the substrate.

Electrochemical reduction of organometallic complexes of rhodium and platinum [147] is used for the synthesis of active species which are useful for regio- and enantioselective olefin hydroformylation:

$$RCH=CH_2 + CO + H_2 \overset{[Pt] \text{ or } [Rh]}{\rightarrow} RCH_2CH_2CHO$$
$$+ RCH(CHO)CH_3 \quad (31)$$
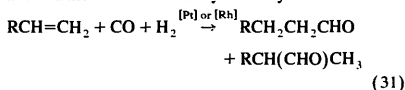
A 98% regioselectivity is obtained for 1-hexene with a Pt–Sn system to produce only the linear aldehyde (1-heptanal). In this case, the complex PtL$_2$Cl$_2$ (in which the ligand is a phosphine derivative) is reduced in the presence of a tin anode to produce new platinum species. The reactions were carried out in a benzene–propylene carbonate mixture. The authors concluded that the nature of the solvent and ligand are critical in these reactions. Dissociated platinum complexes are probably responsible for the regioselectivity. Meanwhile, the role of tin is to abstract chloride anions to produce cationic platinum species.

X = Cl, Br, I
n = 0,1
m = 1, 2

Scheme 12.

Similarly, olefin hydroformylation can be performed on an electrochemically generated rhodium catalyst:

$$Rh(CO)(PPh_3)_2Cl + 2e^-$$
$$\overset{-0.9 \text{ V vs. Ag/AgCl}}{\rightarrow} \left[Rh(CO)(PPh_3)_2\right]^- + Cl^- \quad (32)$$
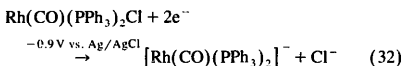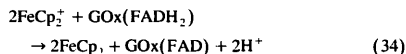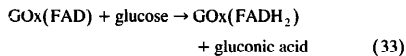
When the triphenylphosphine ligand is replaced by a chiral one, the asymmetric hydroformylation of styrene is achieved with good yields and enantiomeric excess up to 30.9% is obtained.

5. Modified electrodes

We discussed in Section 3 that reactions at the electrode surface can occur rapidly (reversible) or slowly (irreversible) in the time scale of the experiment. As Marcus theory predicts, the difference between these two behaviors arises from the activation energy of the reaction at the electrode surface, since a reaction that requires a minimum structural change of the electroactive species behaves as reversible with a small activation energy which is easily overcome at room temperature. Meanwhile, those electroactive species that involve large structural changes or bond breaking will have a higher activation energy for the same ET process. Sometimes the overpotential needed is larger than the window potential of the solvent. To avoid this problem, redox mediators can be used. These redox mediators are reversible redox systems aimed to decrease the ET activation energy between the electrode and the slowly reactive electroactive species. Redox mediators have to fulfill the following conditions:

1. ET between the electrode and the redox mediator must be fast;
2. ET between the redox mediator and the non-reversible electroactive species must be faster than between the electrode and the non-reversible electroactive species;
3. the oxidized and reduced forms of the mediator should not undergo secondary reactions.

As an example, the catalytic re-oxidation of the enzyme glucose oxidase (GOx) by ferrocene derivatives has been studied extensively [5,148–150]. Eqs. (33)–(35) show the catalytic cycle.

$$GOx(FAD) + glucose \rightarrow GOx(FADH_2)$$
$$+ \text{gluconic acid} \quad (33)$$

$$2FeCp_2^+ + GOx(FADH_2)$$
$$\rightarrow 2FeCp_2 + GOx(FAD) + 2H^+ \quad (34)$$

$$FeCp_2 \rightarrow FeCp_2^+ + e^- \quad (35)$$

GOx oxidizes glucose to gluconic acid through its active center flavin adenine nucleotide (FAD) which is reduced (FADH$_2$), Eq. (33). The active center of GOx,
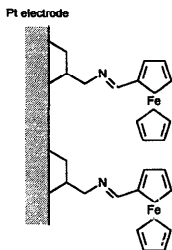
Fig. 8. Modified platinum surface with allylamine ferrocene.

is deeply buried in the structure of GOx with a diameter of 70 Å [151], making impossible the direct ET between the active center and the electrode. The FADH$_2$ therefore must be oxidized by a soluble mediator: ferricenium ion, Eq. (34). The reduced form of the mediator diffuses to the electrode where it is oxidized, Eq. (35).

The electrode should be held at a potential at which the ferrocene is totally oxidized. In this way the resulting current can be related to the glucose concentration.

Modified electrodes break two-dimensional restrictions of bare electrodes, since the surface-attached redox centers are able to produce new arrangements in the transition state. The ET to the electrode surface is then made by reversible electroactive species attached to the electrode surface. A comprehensive review on modified electrodes can be found in the book by Murray [152].

Ferrocene derivatives are by far the most popular of the organometallic compounds used in modified electrodes. They are electrochemically reversible, stable, easy to synthesize and their electrode potentials fall in a potential window that make them useful in practically any solvent.

One of the early examples of an organometallic compound attached to an electrode surface was given by Sharp et al. [2]. These authors modified a platinum surface with allylamine and covalently bound ferrocenecarboxyaldehyde to the amino group as shown in Fig. 8. The voltammetric response observed corresponds
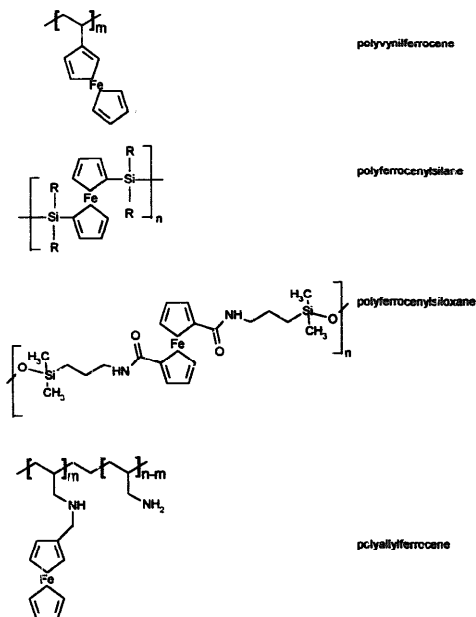

Fig. 9. Examples of ferrocene-based polymers.

to an adsorbed species. Since then there has been a considerable interest in understanding the electronic coupling between the electrode and the electroactive molecular surface site, but it remained poorly understood until Chidsey and co-workers [153,154] incorporated a ferrocene couple at well-defined distances from an electrode. In this case, ferrocene groups were connected to a gold electrode through alkanethiol chains. The electroactive alkanethiol chains were diluted with unsubstituted alkanethiols avoiding interactions among ferrocenes. The resulting chains tilted to achieve the most densely packed structure. This model monolayer is a two-dimensional crystalline solution of electroactive and electroinactive adsorbates. Chidsey and co-workers were able to measure ET rates and to determine the thermal activation and electron tunneling components of this prototypical interfacial ET reaction. This work represents an important step forward in the understanding of heterogenous ET and its control.

The self assembled monolayers (SAMs) are well suited for ET studies and for those reactions where the mediator has to be in a well-defined position. Most of the mediators in solution interact randomly with redox species as explained for ferrocene and GOx. Another way in which it is possible to approximate the behavior of the mediator in solution is to bind the mediator to a surface polymer with a random distribution of the redox centers. If the redox centers are close enough, electrons propagate through the layers of the polymer resembling the behavior of a frozen solution where electrons diffuse instead of ions. The electronic diffusion coefficients by hopping mechanism are lower than diffusion coefficients in solution (ca. 10^{-9}–10^{-11} cm^2 s^{-1} against ca. 10^{-6} cm^2 s^{-1}) but surface concentrations of organometallic mediators can be considerably high (ca. 0.1–1 M). Furthermore, the electronic diffusion coefficient depends on the concentration of redox centers in the polymer; a recent discussion of the charge transport in polymer-modified electrodes was written by Inzelt [155]. There is considerable work on the synthesis of these polymers. Fig. 9 depicts some of the most studied polymers: polyvinylferrocene [156], poly(ferrocenylsilanes) [157,158], polysiloxanes [3,159] and polyallylamine [5]; some of them have technological applications like sensors and electronic devices.

Polyvinylferrocene (PVF) combined with a viologen-polymer have found application as a chemical diode [160]. The viologen-polymer (BPQ) is cathodically deposited on one electrode and polyvinylferrocene on the other. The electrochemical behavior of this structure is shown in Fig. 10. Ideally, current flow should be unidirectional, because the viologen polymer cannot be reduced and polyvinylferrocene can only be oxidized within the available potential window. Thus current flow begins when the potential applied between the two array electrodes is close to the difference between the
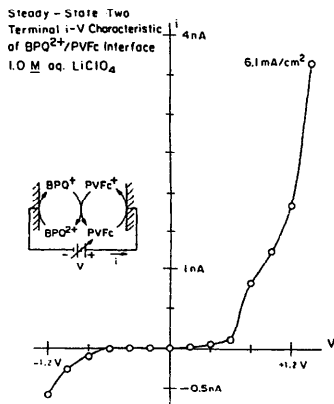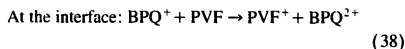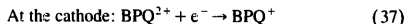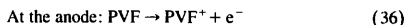

Fig. 10. Two terminal steady-state characteristics of the array of microelectrodes. The right-hand side corresponds to the connections and bias as shown in the inset; the left-hand side, to the opposite bias (PVF side negative). Reprinted from Ref. [160] © American Chemical Society.

standard potentials of the two redox couples, with the occurrence of the following reactions:

At the anode: $PVF \rightarrow PVF^+ + e^-$ (36)

At the cathode: $BPQ^{2+} + e^- \rightarrow BPQ^+$ (37)

At the interface: $BPQ^+ + PVF \rightarrow PVF^+ + BPQ^{2+}$ (38)

When the system is polarized with opposite bias, only a small current flows for the same applied bias potential (ca. 0.9 V); the finite reverse current is likely due to impurities in the water or the onset of water decomposition since Eq. (38) is thermodynamically uphill.

Different ferrocene-based polymers were use to construct biosensors [4,5,161,162]. Fig. 11 depicts the relay mechanism used to sense glucose by ferrocene derivatives as mediators. In our laboratory, polyallylamine
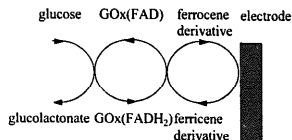

Fig. 11. The ET reactions involved in the determination of glucose by an amperometric device.

ferrocene-modified electrodes have shown high density currents for the amperometric determination of glucose [5] comparable to those obtained with osmium complexes by Heller [163].

Another example of an organometallic compound with electroanalytical application is pentaoxa[13]-ferrocenophane (12), which can bind in its reduced state Group IA metal cations, but releases them in its oxidized state (12$^+$) [164]. For example, when Na$^+$ is coordinated to 12 its potential is shifted by around 200 mV toward anodic potentials. Also, the facility to switch cations on and off has been used [165] to transport alkali metal cations across a liquid membrane containing 12 as the carrier. Several crown ethers combined with ferrocene and other organometallic compounds were synthesized; a review was written by Beer [166].

12   12$^+$
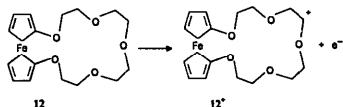
6. Concluding remarks

The work described in this review outlines the trend expected in the future for organometallic electrochemistry. The extensive use of digital simulation and ultrafast CV will allow the elucidation of complex organometallic reaction mechanisms. The advances in spectroelectrochemistry will produce an important impact in the understanding of the molecular structure of very reactive and unstable intermediates in organometallic chemistry.

The selectivity and efficiency of ET-catalyzed reactions have a strong potential for the alternative synthesis of organometallic compounds with chiral properties. The electrochemical generation of catalysts for regioselective synthesis evolves as a promising field.

The use of organometallics in electrochemically based sensors and molecular devices are a reality [2] and further uses in molecular electronics are expected.

---

[2] Exactech blood glucose meter, Medisense, Inc., Waltham, MA 02154, USA.

References

[1] J.A. Page, G. Wilkinson, J. Am. Chem. Soc. 74 (1952) 6149.
[2] M. Sharp, M. Peterson, K. Edström, J. Electroanal. Chem. 95 (1979) 12.
[3] C.M. Casado, M. Morán, J. Losada, I. Cuadrado, Inorg. Chem. 34 (1995) 1668 and references cited therein.
[4] H. Bu, S.R. Mikkelsen, A.M. English, Anal. Chem. 67 (1995) 4071.
[5] E.J. Calvo, C. Danilowicz, L. Díaz, J. Electroanal. Chem. 369 (1994) 279.
[6] M.D. Morris, in: A.J. Bard (Ed.), Electroanalytical Chemistry: A Series of Advances, vol. 7, Marcel Dekker, New York, 1974, p. 79.
[7] D. De Montauzon, R. Poilblanc, P. Lemoine, M. Gross, Electrochim. Acta 23 (1978) 1247.
[8] N.G. Connelly, W.E. Geiger, Adv. Organomet. Chem. 23 (1984) 1.
[9] A. Vlcek Jr., Chemtracts Inorg. Chem. 5 (1993) 1.
[10] D.H. Evans, Chem. Rev. 90 (1990) 739.
[11] W.E. Geiger, Acc. Chem. Res. 28 (1995) 351.
[12] A.M. Vecchio-Sadus, J. Appl. Electrochem. 23 (1993) 401.
[13] M.D. Ryan, E.F. Bowden, J.Q. Chambers, Anal. Chem. 66 (1994) 360R.
[14] A.J. Bard, L. Faulkner, Electroanalytical Methods, Wiley, New York, 1980.
[15] P.T. Kissinger, W.R. Heineman (Eds.), Laboratory Techniques in Electroanalytical Chemistry, Marcel Dekker, New York, 1984.
[16] P.H. Rieger, Electrochemistry, Chapman and Hall, New York, 1993.
[17] R.S. Nicholson, I. Shain, Anal. Chem. 36 (1964) 706.
[18] B.R. Scharifker, in: J.O'M. Bockris (Ed.), Modern Aspects of Electrochemistry, vol. 22, Plenum, New York, 1992, p. 467.
[19] R.M. Wightman, D.O. Wipf, in: A.J. Bard (Ed.), Electroanalytical Chemistry: A Series of Advances, vol. 15, Marcel Dekker, New York, 1989.
[20] R.M. Wightman, D.O. Wipf, Acc. Chem. Res. 23 (1990) 64.
[21] A.M. Bond, R. Colton, J.B. Cooper, J.C. Traeger, J.N. Water, D.M. Way, Organometallics 13 (1994) 3434.
[22] J. Heinze, Angew. Chem. Int. Ed. Engl. 32 (1993) 1269.
[23] I. Cassidy, S.B. Khoo, S. Pons, M. Fleischmann, J. Phys. Chem. 89 (1985) 3933.
[24] B. Sharifker, G. Hills, J. Electroanal. Chem. 130 (1981) 81.
[25] L.S. Maia, M.J. Medeiros, M.I. Montenegro, D. Court, D. Pletcher, J. Electroanal. Chem. 164 (1984) 347.
[26] A.S. Baranski, J. Electrochem. Soc. 133 (1986) 93.
[27] L.M. Abrantes, M. Fleischman, L.M. Peter, S. Pons, B.R. Sharifker, J. Electroanal. Chem. 164 (1984) 347.
[28] S.W. Feldberg, C. Averbach, Anal. Chem. 36 (1964) 505.
[29] S.W. Feldberg, in: A.J. Bard (Ed.), Electroanalytical Chemistry: A Series of Advances, vol. 3, Marcel Dekker, New York, 1969, p. 199.
[30] D. Britz, Digital Simulation in Electrochemistry, Springer-Verlag Berlin, 1988.
[31] J. Heinze, J. Electroanal. Chem. 124 (1981) 73.
[32] J. Heinze, Ber. Bunsenges. Phys. Chem. 85 (1981) 1096.
[33] J. Heinze, M. Storzbach, Ber. Bunsenges. Phys. Chem. 90 (1986) 1043.

[34] ELSIM, Electrochemistry Software Library, Technical Software Distribution, Charlotte, NC.

[35] DIGISIM, Bioanalytical Systems, Inc., West Lafayette, IN.

[36] M. Rudolph, E.P. Reddy, S.W. Feldberg, Anal. Chem. 66 (1994) 589A.

[37] R.L. McCreery, Prog. Anal. Spectrosc. 11 (1988) 141.

[38] J. Robinson, Spectroelectrochemistry, in: Specialist Periodical Report, Electrochemistry, vol. 9, The Royal Society, London, 1983, p. 101.

[39] R.J. Gale (Ed.), Spectroelectrochemistry, Theory and Practice, Plenum, New York, 1988.

[40] R.P. Van Duyne, T.H. Ridway, C.N. Reilley, J. Electroanal. Chem. 69 (1976) 165.

[41] F. Battaglini, E.J. Calvo, J. Electroanal. Chem. 240 (1990) 443.

[42] R.W. Murray, W.R. Heinemann, G.W. O'Dom, Anal. Chem. 39 (1967) 1666.

[43] J.R. Pugh, T.J. Meyer, J. Am. Chem. Soc. 114 (1992) 3784.

[44] M.B.G. Pilkington, B.A. Coles, R.G. Compton. Anal. Chem. 61 (1989) 1787.

[45] R.G. Compton, R.G. Wellington, J. Phys. Chem. 98 (1994) 270.

[46] R.G. Compton, H.C. Fislcher, R.G. Wellington, J. Winkler, J. Phys. Chem. 96 (1992) 8153.

[47] R.G. Compton, J. Winkler, D.J. Riley, S.D. Bearpark, J. Phys. Chem. 98 (1994) 6818.

[48] A.M. Waller, R.G. Compton, in: R.G. Compton (Ed.), Comprehensive Chemical Kinetics, vol. 29, Elsevier, Amsterdam, 1989.

[49] W. Kaim, R. Reinhart, M. Sieger, Inorg. Chem. 33 (1994) 4453.

[50] R.N. Bagchi, A.M. Bond, R. Colton, I. Creece, K. McGregor, T. Whyte, Organometallics 10 (1991) 2611.

[51] C.A. Ghilardi, F. Laschi, S. Midollini, A. Orlandini, G. Scapacci, P. Zanello, J. Chem. Soc. Dalton Trans. (1995) 531.

[52] D.L. Du Bois, J.A. Turner, J. Am. Chem. Soc. 104 (1982) 4989.

[53] J.D. Roth, M.J. Weaver, Anal. Chem. 63 (1991) 1603.

[54] C.A. Blaine, J.E. Ellis, K.R. Mann, Inorg. Chem. 34 (1995) 1552.

[55] G.J. Lewis, J.D. Roth, R.A. Montag, L.K. Safford, X. Gao, S.C. Chang, L.F. Dahl, M.J. Weaver, J. Am. Chem. Soc. 112 (1990) 2831.

[56] W. Bruns, W. Kaim, E. Waldhor, M. Krejcik, Inorg. Chem. 34 (1995) 663.

[57] E. Laviron, J. Electroanal. Chem. 109 (1980) 57.

[58] E. Laviron, J. Electroanal. Chem. 124 (1981) 1.

[59] E. Laviron, J. Electroanal. Chem. 124 (1981) 9.

[60] E. Laviron, J. Electroanal. Chem. 130 (1981) 23.

[61] E. Laviron, J. Electroanal. Chem. 134 (1982) 205.

[62] E. Laviron, J. Electroanal. Chem. 137 (1982) 1.

[63] E. Laviron, J. Electroanal. Chem. 146 (1983) 1.

[64] E. Laviron, J. Electroanal. Chem. 146 (1983) 15.

[65] E. Laviron, L. Roullier, J. Electroanal. Chem. 157 (1983) 7.

[66] E. Laviron, J. Electroanal. Chem. 169 (1984) 23.

[67] E. Laviron, J. Electroanal. Chem. 169 (1984) 29.

[68] E. Laviron, L. Roullier, J. Electroanal. Chem. 186 (1985) 1.

[69] E. Laviron, J. Electroanal. Chem. 208 (1986) 357.

[70] M. Mastrogostino, L. Nadjo, J.M. Saveant, Electrochem. Acta 13 (1968) 721.

[71] C. Amatore, J.M. Saveant, J. Electroanal. Chem. 85 (1977) 27.

[72] C. Amatore, J.M. Saveant, J. Electroanal. Chem. 86 (1977) 227.

[73] C. Amatore, J.M. Saveant, J. Electroanal. Chem. 102 (1979) 21.

[74] C. Amatore, J.M. Saveant, J. Electroanal. Chem. 107 (1980) 353.

[75] C. Amatore, J.M. Saveant, J. Electroanal. Chem. 123 (1981) 189.

[76] C. Amatore, J.M. Saveant, J. Electroanal. Chem. 123 (1981) 203.

[77] C. Amatore, F. M'Halla, J.M. Saveant, J. Electroanal. Chem. 123 (1981) 219.

[78] C. Amatore, J. Pinson, J.M. Saveant, A. Thiebault, J. Electroanal. Chem. 123 (1981) 231.

[79] C. Amatore, J.M. Saveant, J. Electroanal. Chem. 125 (1981) 1.

[80] C. Amatore, J.M. Saveant, J. Electroanal. Chem. 125 (1981) 23.

[81] C. Amatore, J.M. Saveant, J. Electroanal. Chem. 126 (1981) 1.

[82] J.G. Gaudiello, T.C. Wright, R.A. Jounes, A.J. Bard, J. Am. Chem. Soc. 107 (1985) 888.

[83] R.D. Moulton, D.J. Chandler, A.M. Arif, R.A. Jounes, A.J. Bard, J. Am. Chem. Soc. 110 (1988) 5714.

[84] D.J. Kuchynka, J.K. Kochi, Organometallics 8 (1989) 677.

[85] D.J. Kuchynka, J.K. Kochi, Inorg. Chem. 27 (1988) 2574.

[86] A. Vallat, M. Person, L. Roullier, E. Laviron, Inorg. Chem. 26 (1987) 332.

[87] R.G. Compton, R. Barghout, J.C. Eklund, A.C. Fisher, A.M. Bond, R. Colton, J. Phys. Chem. 97 (1993) 1661.

[88] R. Colton, A.M. Bond, M.J. McCormick, Inorg. Chem. 16 (1977) 155.

[89] R.G. Compton, R.A.W. Dryfe, Prog. React. Kinet. 20 (1995) 245.

[90] J. Moraczewski, W.E. Geiger, J. Am. Chem. Soc. 101 (1979) 3407

[91] W.E. Geiger, T. Gennett, M. Grzeszczuk, G.A. Lane, J. Moraczewski, A. Salzer, D.E. Smith, J. Am. Chem. Soc. 108 (1986) 7454.

[92] R.L. Rich, H. Taube, J. Am. Chem. Soc. 76 (1954) 2608.

[93] F. Basolo, R.G. Pearson, Mechanisms of Inorganic Reactions, Wiley, New York, 1967.

[94] S.W. Feldberg, L.J. Jeftic, J. Phys. Chem. 76 (1972) 2439.

[95] J.W. Hershberger, R.J. Kingler, J.K. Kochi, J. Am. Chem. Soc. 105 (1983) 61.

[96] J.M. Mevs, W.E. Geiger, J. Am. Chem. Soc. 111 (1989) 1922.

[97] J. Moraczewski, W.E. Geiger, J. Am. Chem. Soc. 111 (1989) 2096.

[98] A.M. Bond, D.J. Darensbourg, E. Mocellin, B.J. Stewart, J. Am. Chem. Soc. 103 (1981) 6827.

[99] A.M. Bond, S.W. Carr, R. Colton, Organometallics 3 (1984) 541.

[100] A.M. Bond, S.W. Carr, R. Colton, Inorg. Chem. 23 (1984) 2343.

[101] R.H. Philip, D.L. Reger, A.M. Bond, Organometallics 8 (1989) 1714.

[102] A.M. Bond, R. Colton, J.F. Kevekordes, Inorg. Chem. 25 (1986) 749.

[103] K.A. Conner, R.A. Walton, Inorg. Chem. 25 (1986) 4422.

[104] N.G. Connelly, S.J. Raven, G.A. Carriedo, V.J. Riera, J. Chem. Soc. Chem. Commun. (1986) 992.

[105] C. Moinet, E. Roman, D. Astruc, J. Electroanal. Chem. 121 (1981) 241.

[106] A. Darchen, J. Organomet. Chem. 302 (1986) 389.

[107] G.J. Bezems, P.H. Rieger, S. Visco, J. Chem. Soc. Chem. Commun. (1981) 265.

[108] M. Arewgoda, P.H. Rieger, B.H. Rieger, J. Simpson, S.J. Visco, J. Am. Chem. Soc. 104 (1982) 5633.

[109] M.G. Richmond, J.K. Kochi, Inorg. Chem. 25 (1986) 656.

[110] M.G. Richmond, J.K. Kochi, Organometallics 6 (1987) 254.

[111] H.H. Ohst, J.K. Kochi, J. Am. Chem. Soc. 108 (1986) 2897.

[112] F. Marken, A.M. Bond, R. Colton, Inorg. Chem. 34 (1995) 1705.

[113] T. Roth, W. Kaim, Inorg. Chem. 31 (1992) 1930.

[114] C. Amatore, A. Jutand, Acta Chem. Scand. 44 (1990) 755.

[115] C. Amatore, A. Jutand, A. Suarez, J. Am. Chem. Soc. 115 (1993) 9531.

[116] C. Amatore, A. Jutand, Organometallics 7 (1988) 2203.

[117] T.T. Tsou, J.K. Kochi, J. Am. Chem. Soc. 101 (1979) 6319.

[118] M. Troupel, Y. Rollin, S. Sibille, J.F. Fauvarque, J. Perichon, J. Chem. Res. (S) (1980) 24.

[119] D.M. Wayner, V.D. Parker, Acc. Chem. Res. 26 (1993) 287.

[120] M. Tilset, V.D. Parker, J. Am. Chem. Soc. 111 (1989) 6711; J. Am. Chem. Soc. 112 (1990) 2843.

[121] V.D. Parker, K.L. Handoo, F. Roness, M. Tilset, J. Am. Chem. Soc. 113 (1991) 7493.

[122] T. Aase, V.D. Parker, M. Tilset, J. Am. Chem. Soc. 112 (1990) 4974.

[123] V. Skagestad, M. Tilset, J. Am. Chem. Soc. 115 (1993) 5077.

[124] E.J. Calvo, in: C.H. Branford, R.G. Compton (Eds.), Comprehensive Chemical Kinetics, vol. 26, Elsevier, Amsterdam, 1986, p. 1.

[125] D.G. Tuck, in: A.J.L. Pombeiro and J.A. McCleverty (Eds.), Molecular Electrochemistry of Inorganic, Bioinorganic and Organometallic Compounds, Kluwer, Netherlands, 1993, p. 15.

[126] J. Grobe, Comments Inorg. Chem. 9 (1990) 149.

[127] F.F. Said, D.G. Tuck, Can. J. Chem. 58 (1980) 1673.

[128] J.J. Habeeb, A. Osman, D.G. Tuck, J. Organomet. Chem. 185 (1980) 117.

[129] F.F. Said, D.G. Tuck, J. Organomet. Chem. 224 (1982) 121.

[130] P.C. Hayes, A. Osman, N. Seudeal, D.G. Tuck, J. Organomet. Chem. 291 (1985) 1.

[131] J.J. Habeeb, F.F. Said, D.G. Tuck, J. Organomet. Chem. 190 (1980) 325.

[132] J.S. Banait, P.K. Pahil, Bull. Electrochem. 5 (1989) 264.

[133] J.S. Banait, P.K. Pahil, Bull. Electrochem. 3 (1987) 237.

[134] J. Grobe, B.H. Schneider, H. Zimmermann, Z. Anorg. Allg. Chem. 481 (1981) 107.

[135] L. Shirokii, N.A. Maier, Yu.A. Ol'dekop, Vestsi Akad. Navuk BSSR Ser. Khim. Navuk (1986) 106; Chem. Abstr. 105 (1986) 160779a.

[136] R. Yin, Hauxue Shijie 28 (1987) 170; Chem. Abstr. 107 (1987) 66416z.

[137] D. Astruc, Angew. Chem. 100 (1988) 662; Angew. Chem. Int. Ed. Engl. 27 (1988) 643.

[138] D. Astruc, Electron Transfer and Radical Processes in Transition Metal Chemistry, VCH, New York, 1995.

[139] J.K. Kochi, J. Organomet. Chem. 300 (1986) 139.

[140] M. Chanon, Acc. Chem. Res. 20 (1987) 214.

[141] J.W. Hershberger, R.J. Klingler, J.K. Kochi, J. Am. Chem. Soc. 104 (1982) 3034.

[142] E.K. Lhadi, C. Mahe, H. Patin, A. Darchen, J. Organomet. Chem. 246 (1983) C61.

[143] A. Darchen, E.K. Lhadi, H. Patin, J. Organomet. Chem. 259 (1983) 189.

[144] S. Sibille, E. d'Incan, L. Leport, M.-C. Massebiau, J. Périchon, Tetrahedron Lett. 28 (1987) 55.

[145] S. Durandetti, S. Sibille, J. Périchon, J. Org. Chem. 54 (1989) 2198.

[146] S. Olivero, J.C. Clinet, E. Duñach, Tetrahedron Lett. 36 (1995) 4429.

[147] A. Mortreux, F. Petit, Adv. Chem. Ser. 230 (1992) 261.

[148] A.E.G. Cass, G. Davis, G.D. Francis, H.A.O. Hill, W.J. Astor, I.J. Higgins, E.V. Plotkin, L.D.L. Scott, A.P.F. Turner, Anal. Chem. 56 (1984) 667.

[149] Y. Degani, A. Heller, J. Phys. Chem. 91 (1987) 1285.

[150] A. Badia, R. Carlini, A. Fernandez, F. Battaglini, S. Mikkelsen, A. English, J. Am. Chem. Soc. 115 (1993) 7053.

[151] H.J. Hecht, H.M. Kalisz, J. Hendle, R.D. Schmid, D. Schomburg, J. Mol. Biol. 229 (1993) 153.

[152] R. Murray, Molecular Design of Electrodes, Techniques of Chemistry, vol. 22, Wiley, New York, 1992.

[153] C.E.D. Chidsey, C.R. Bertozzi, T.M. Putvinski, A.M. Mujsce, J. Am. Chem. Soc. 112 (1990) 4301.

[154] C.E.B. Chidsey, Science 251 (1991) 919.

[155] G. Inzelt, in: A.J. Bard (Ed.), Electroanalytical Chemistry: A Series of Advances, vol. 18, Marcel Dekker, New York, 1994, p. 89.

[156] A. Merz, A.J. Bard, J. Am. Chem. Soc. 100 (1978) 3222.

[157] D.A. Foucher, B.Z. Tang, I. Manners, J. Am. Chem. Soc. 114 (1992) 6246.

[158] M.T. Nguyen, A.F. Diaz, V.V. Dement'ev, K.H. Pannel, Chem. Mater. 5 (1993) 1389.

[159] C.M. Casado, I. Cuadrado, M. Morán, B. Alonso, F. Lobete, J. Losada, Organometallics 14 (1995) 2618.

[160] G.P. Kittlesen, H.S. White, M.S. Wrighton, J. Am. Chem. Soc. 107 (1985) 7373.

[161] S.P. Hendry, M.F. Cardosi, A.P.F. Turner, Anal. Chim. Acta 281 (1993) 453.

[162] P.D. Hale, L.I. Boguslavsky, T. Inagaki, H.I. Karan, H.S. Lee, T.A. Skotheim, Y. Okamoto, Anal. Chem. 63 (1991) 677.

[163] A. Heller, Acc. Chem. Res. 23 (1990) 128.

[164] T. Saji, Chem. Lett. (1986) 275.

[165] T. Saji, I. Kinoshita, J. Chem. Soc. Chem. Commun. (1986) 715.

[166] P.D. Beer, Endeavour 16 (1992) 182.